About the Kinetic Feasibility of the Lipscomb Mechanism in Human Carbonic Anhydrase II

Christofer S. Tautermann,[‡] Markus J. Loferer,[†] Andreas F. Voegele,[†] and Klaus R. Liedl*[,†]

Institute of General, Inorganic and Theoretical Chemistry, University of Innsbruck, Innrain 52a, A-6020 Innsbruck, Austria, and Institute of Computer Science, University of Innsbruck, Technikerstrasse 27, A-6020 Innsbruck, Austria

Received: May 19, 2003; In Final Form: August 4, 2003

The active site of carbonic anhydrase II is investigated by a widely used model system ($[Zn(NH_3)_3(HCO_3)(H_2O)_n(CH_3OH)_m]^+$, $n = 0, 1, 2$ and $m = 0, 1$) to explore the proton transfer within zinc-bound bicarbonate by quantum chemical methods. This proton transfer is a key step in the reversible hydration reaction of carbon dioxide, and although it is not the rate-limiting step in the overall reaction, its mechanism is heavily debated. Kinetic data of the system are computed by variational transition-state theory with tunneling corrections based on high-level quantum chemical methods such as coupled cluster and Gaussian-3 variants. From our data, it can be concluded that the proton transfer in Lipscomb fashion involves at least one proton-transfer-mediating water molecule, and the Thr199 is shown to play a key role as proton donor/acceptor entity, especially in the backward reaction (the dehydration of bicarbonate). The availability of the hydroxy group of Thr199 has been approved by a 50 ps semiempirical QM/MM simulation. The uncatalyzed proton transfer in the hydration reaction reveals a reaction barrier of more than 30 kcal/mol. If catalyzed by one water molecule and the OH-group of threonine, this barrier decreases to less than 10 kcal/mol. The catalyzed model reaction is shown to yield reaction rates of more than 10^8 s^{-1}, thus being much faster than the rate-limiting step of the carbon dioxide conversion by carbonic anhydrase II. Our results therefore do not rule out the Lipscomb mechanism as a possible proton-transfer step, in contrast to various other studies, in which it is rejected with energetic arguments. Tunneling is shown to have significant effects in this part of the catalytic cycle even at room temperature by enhancing the reaction rate by more than 1 order of magnitude.

1. Introduction

The human carbonic anhydrases (HCAs) form a family of several zinc metalloenzymes, which are of essential biological importance in respiration and photosynthesis and as physiological buffers.[1−7] The enzyme catalyzes the reversible hydration reaction of carbon dioxide

$$CO_2 + H_2O \rightleftharpoons HCO_3^- + H^+ \qquad (1)$$

The hydration reaction of carbon dioxide is accelerated by a factor 10^7, yielding a turnover of about 10^6 s^{-1} at room temperature, which is a reaction rate close to the diffusion limit.[8] The structure of the enzyme (and many variants) was determined by high-resolution X-ray spectroscopy.[9−12] In the active site of HCA II, the catalytically required Zn^{2+} atom is coordinated by three histidine residues (i.e., His94, His96, and His119) at the bottom of a 15 Å deep cavity. Including the fourth ligand (i.e., water or hydroxide, depending on the pH) reveals a slightly disturbed tetrahedral coordination. Another important feature of the active site is Thr199, which forms hydrogen bonds to zinc-bound ligands and to Glu106.[13−16] In the cavity, a hydrogen-bond network between a group of several (up to six) water molecules[17] interacting tightly with the above-mentioned residues are proposed to be responsible for the proton transfer into the bulk solution via His64.[10,18−20]

The catalytic mechanism of carbonic anhydrase II (CA II) has been investigated in many studies, both theoretically[15,21−28] and experimentally.[2,3,29−32] The most widely accepted catalytic mechanism for the enzymatic activity of carbonic anhydrase may be described by three distinct steps: First the zinc-bound water has to be deprotonated, and the proton has to be transferred to the bulk solution. This is regarded as the rate-limiting step and involves several water molecules in the cavity, as well as the His64 at the outermost part of the cavity.[2,15,22,24,33,34] This deprotonation yields the catalytically active zinc-hydroxide species, which now may react with carbon dioxide to yield zinc-bound bicarbonate. This reaction has been studied by Solá et al.,[21] Zheng et al.,[35] Muguruma,[25] and recently Cui and Karplus[28] by means of computational chemistry.

It is generally accepted that the primarily formed bicarbonate complex has to be modified to become a better leaving group. The proton of the bicarbonate molecule has to migrate from the zinc-bound oxygen to that oxygen of the bicarbonate entity furthest away from the zinc ion to transform the bicarbonate into a better leaving group. To accomplish this rearrangement, several different mechanisms have been proposed, and the two most prominent ones are the *Lipscomb* and the *Lindskog* mechanisms.[26] The first mechanism suggests that the proton is physically transferred from one oxygen to the other one, whereas the second mechanism proposes a semirotation of the whole bicarbonate entity to yield the desired (but permuted) structure (see Figure 1). In the last step of the reaction, the bicarbonate gets substituted by water and the catalytic cycle begins again.[36]

Many studies have extensively discussed the theoretical possibilities of both mechanisms,[21,23,25−27] and different conclusions were drawn: Muguruma[25] and Bräuer et al.[27] followed from their studies that the Lindskog and the Lipscomb mech-

* Corresponding author.
‡ Institute of Computer Science.
† Institute of General, Inorganic and Theoretical Chemistry.

10.1021/jp0353789 CCC: $25.00
Published on Web 10/03/2003

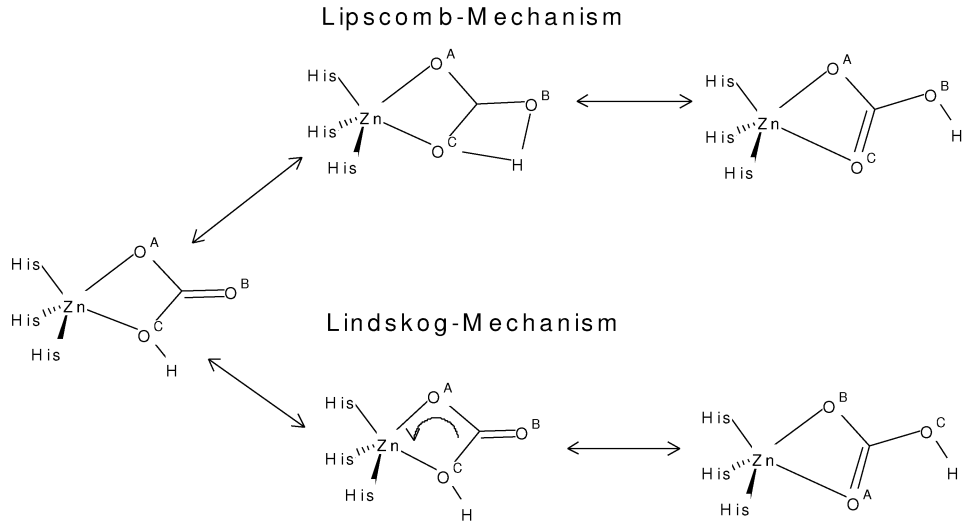

Figure 1. Schematic representation of the two concurring mechanisms for the proton transfer in the bicarbonate entity in carbonic anhydrase. Although the products are chemically equivalent, they are formally not the same because the oxygen atoms are permuted.

anisms are competitive mechanisms, whereas Hartmann et al.[23] and Mauksch et al.[26] found the Lindskog mechanism to be preferred for energetic reasons.

Until now, computational studies have focused their attention mainly on the energetics of the various single steps in the entire catalytic cycle. Because it is not feasible to calculate the whole enzyme by ab initio methods, simplifications have to be introduced by considering only the active site by quantum chemical methods. Several systems have been used to model the active site of carbonic anhydrase. Hartmann at al.[23] used an $[\text{imidazole}_3\text{Zn(OH)}]^+ \cdot \text{CO}_2$ complex and a semiempirical approach. Muguruma,[25] Mauksch et al.,[26] Bräuer et al.,[27] and Isaev[34] used a slightly smaller system, in which the imidazoles are substituted by ammonia. Other residues besides the zinc-coordinating ones were also included, described by small molecules (methanol to model Thr199 and ammonia to model His64), and ab initio methods to evaluate the energetics of the stationary points (i.e., the minima and transition states) were applied. From these studies, one learns the great benefit of model systems, and we chose to use a similar model system to determine the energetics at a high ab initio level, as well as the kinetics of the proton-transfer step following the Lipscomb mechanism. Although there have been attempts to evaluate the energetics of the catalytic cycle by ab initio methods, the highest level of theory was a perturbational approach of second order (MP2) by Muguruma.[25] Our approach is to determine the energy differences in the model system by coupled cluster and Gaussian-3 methods to yield reliable values. Because the energy barriers are used to determine the kinetics of the systems, it is very important to keep the error very small because an error of 1.5 kcal/mol in the barrier leads to an error of 1 order of magnitude in the reaction rate (at room temperature).

The aim of this study is the thorough kinetic investigation of the Lipscomb mechanism. Although Hartmann et al.[23] claim that this mechanism is energetically more demanding,[23] we believe that the transfer of the hydrogen is mediated by water, thus lowering the energy barrier.[21] When considering the proton transfer in similar systems like carbonic acid, it was recently shown that the energy barriers drop vastly when water acts as catalyst, and also tunneling was found to have a big impact on the reaction rate.[37,38] Muguruma[25] has already included one catalytic water entity in the model system, leading to an activation barrier of 8.5 kcal/mol (at the MP2 level of theory), which is about a third of the uncatalyzed barrier (28.3 kcal/mol). In the study by Hartmann et al.,[23] the effect of some surrounding amino acid residues was taken into account, and it was shown that Thr199 plays an important role in the catalytic process.[13−16,39,40] Thus, we decided to include water, as well as methanol (as model for the hydroxy residue of Thr199), as catalysts in our system to estimate the importance of the various catalytic effects. A semiempirical QM/MM simulation of CA II shows that the hydrogen bond between Thr199 and Glu106 undergoes strong fluctuations and is therefore available as catalytic species in the reaction and justifies the inclusion of methanol in the model system. One drawback of these models is the neglect of the surrounding enzymatic environment, but we propose that a model system yields significant results for our purpose. In this study, we want to compare different mechanisms for one single step in the catalytic cycle in CA II, and the neglected surrounding is expected to be quite unchanged during a proton-transfer process.

2. Methods

2.1. The Model System. In analogy to several other studies,[25−27,34] the active site of carbonic anhydrase II is modeled by a zinc atom that is surrounded by three ammonia molecules, which mimic the three coordinating histidines. The orientation of the zinc-bound bicarbonate is chosen such that there is just little interaction by hydrogen bonding between the bicarbonate oxygens and the ammonia hydrogens. The (dotted) distance, −C═O···H−N−, is larger than 2.3 Å in all model systems, and the O−H−N angle is always smaller than 126°, which is a too long distance together with a too small angle to enable strong hydrogen bonds. As already mentioned, the Thr199 is modeled by a methanol molecule, in which the distance between the methanol oxygen and the bicarbonate carbon ranges from 3.39 to 3.74 Å (in the course of the proton-transfer reaction). The X-ray structure of a Thr200 → His mutant of carbonic anhydrase by Xue et al.[12] at a resolution of 1.9 Å reveals a distance of 3.5 Å, which is in good agreement because the authors estimate the error in the atomic coordinates to be ±0.16 Å. The distance between the zinc and the coordinating histidines is found to be 2.16−2.18 Å in the crystal structure, and the distance between zinc and ammonia in our model system varies from 2.12 to 2.18 Å. Thus the position of the methanol molecule and the ammonia entities agrees well with the experimental X-ray structure. A graphical representation of the model with corresponding atom labels is shown in Figure 2.

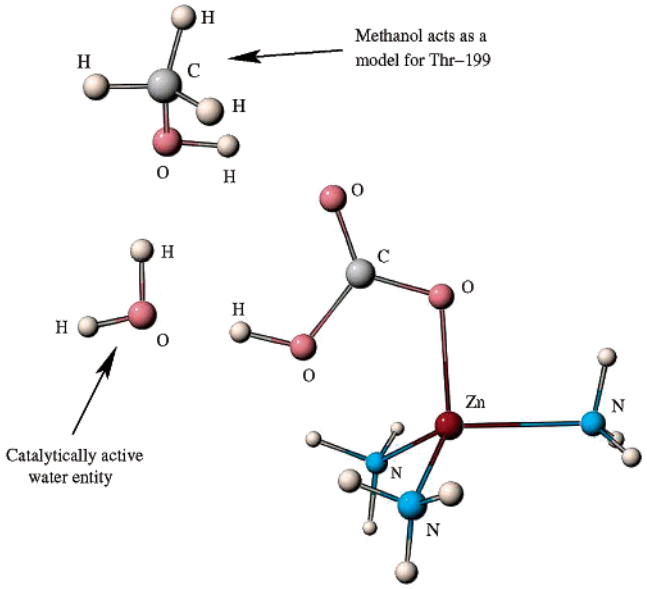

Figure 2. Example of the model systems with assigned atom types.

TABLE 1: Reaction Barriers (in kcal/mol) for the Proton Transfer in the Hydration Reaction of Carbon Dioxide (Denoted by "Forward") and in the Dehydration Reaction of Bicarbonate (Denoted by "Backward") in the Model System at Various Levels of Theory[a]

	B3LYP		G3(MP2)$_{LanL2DZ}$		CCSD(T)	
	forward	backward	forward	backward	forward	backward
+0 H_2O	31.1	40.2	30.7	40.4	30.8	40.3
+1 H_2O	10.7	16.4	12.1	18.0		
+2 H_2O	9.4	15.8	11.9	19.0		
+1 H_2O + CH_3OH	7.6	12.9	9.3	14.3		

[a] B3LYP stands for the B3LYP method using the 6-31+G(d) basis for all atoms but zinc, for which the LanL2DZ basis including the ECPs is applied. G3(MP2)$_{LanL2DZ}$ denotes the G3(MP2) variant that was used in this study, and CCSD(T) stands for CCSD(T)/aug-cc-pVDZ (LanL2DZ and ECPs for Zn)//MP2/aug-cc-pVDZ (LanL2DZ and ECPs for Zn).

2.2. Quantum Chemical Methods. For the determination of the stationary points, we used a somewhat altered Gaussian-3 method.[41−43] The Gaussian-3 theory using reduced Møller−Plesset order (G3(MP2))[44] was slightly modified to be capable of dealing with effective core potentials (ECP) for the zinc atom in our model system. Thus we applied the Los Alamos LanL2DZ basis set with ECPs to the zinc atom. The modified method is now termed G3(MP2)$_{LanL2DZ}$. To validate this subtle change in the G3(MP2) method, we calculated the energy differences of the stationary points by coupled cluster methods with single and double excitation and perturbed triples contributions (CCSD(T)). Dunning's augmented correlation-consistent double-ζ basis (aug-cc-pVDZ) was used for all atoms except zinc, for which again the LanL2DZ basis with ECPs was applied. The coupled cluster single-point energies were computed on MP2-optimized geometries (with the same basis) and are reported in Table 1. The small value for the T1-diagnostic[45] (less than 0.016 for all stationary points) showed that the single-determinant approach for the wave function is appropriate. The energy barriers calculated by the coupled cluster approach are well reproduced (difference of 0.1 kcal/mol) by our G3(MP2)$_{LanL2DZ}$ method, see Table 1.

2.3. Variational Transition-State Theory. We applied the variational approach to transition-state theory[46−53] including quantum chemical effects such as tunneling and corner cutting to calculate the reaction rates. In the framework of this theory, entropic effects are included by choosing the generalized transition state at the point of highest free energy along the reaction path. The potential energy surface (PES) is calculated at a lower level of theory by employing the hybrid density functional method B3LYP using the 6-31+G(d) basis set for all atoms except zinc, for which the LanL2DZ basis set with ECPs was applied. Because DFT is known to reproduce results of high-level methods quite well,[54] the points yield a qualitatively correct description of the reaction swath. Table 1 shows the good correspondence of the DFT energy values to those of the high-level methods. The minimum energy path (MEP), which is the path of least energy connecting products and reactants in internal mass-weighted coordinates, is determined using the Page−McIver method.[55,56] The step size in mass-scaled coordinates (scaled to 1 amu) was set to 0.025 au for the first 60 steps in each direction departing from the transition state, and further away from the transition state, it was set to 0.075 au. Second derivatives of the potential energy in respect to the coordinates were calculated every third step. The PES is interpolated to the three high-level stationary points (i.e., the reactants, the transition state, and the products) according to an interpolation scheme, which also maps the moments of inertia onto the high-level data.[57]

2.4. Tunneling Corrections. Quantum chemical corrections have been applied to the variational transition-state theory (VTST). We used two different approaches of taking into account tunneling contributions in the framework of the semiclassical theory:[58] (1) the small curvature tunneling approach[51,59,60] (SCT), which allows moderate corner cutting along a curved MEP and (2) the large curvature tunneling approach[49] (LCT), which leads to tunneling paths far off the MEP in the nonadiabatic region. As the large curvature method, we employed the LCG4 method to include anharmonicity of the reaction valley[61] in the tunneling calculations.[62] Because both methods, LCT and SCT, perform well in quite different situations, mostly depending on the temperature and the masses of the atoms involved in the tunneling process, the optimum is to use the larger tunneling correction of the two. This is called the microcanonical optimized multidimensional tunneling method (μOMT),[63] which is an excellent approach for including tunneling corrections over the full temperature range.

All stationary points were determined with the Gaussian 98 package,[64] and the kinetics calculations were performed with Polyrate[65] and Gaussrate,[66] being an interface between Gaussian 98 and Polyrate.

2.5. QM/MM Methods. The QM section, which was treated by the semiempirical PM3 Hamiltonian, comprised the three zinc-coordinating histidines, zinc, and bicarbonate. QM/MM boundaries were handled by link atoms, which cut across the bonds between the imidazole side chains and the backbones of His94, His96, and His119. For all residues that were not part of the QM region, standard parameters were used as implemented in the Charmm force field.[67]

Standard simulation protocols were employed including a Langevin setup and a time step of 0.5 fs. A stochastic boundary setup was used.[68] All atoms confined in a sphere of 12 Å radius were treated by QM/MM molecular dynamics (reaction zone), whereas the atoms outside this sphere up to a shell with a radius of 16 Å were treated by stochastic dynamics,[69−71] and the atoms outside of that were kept fixed. Conventional friction constants were employed, and the system was heated to room temperature in the initial few picoseconds.

As the starting structure, the 1.54 Å resolution X-ray structure of human carbonic anhydrase II complexed with bicarbonate[10]

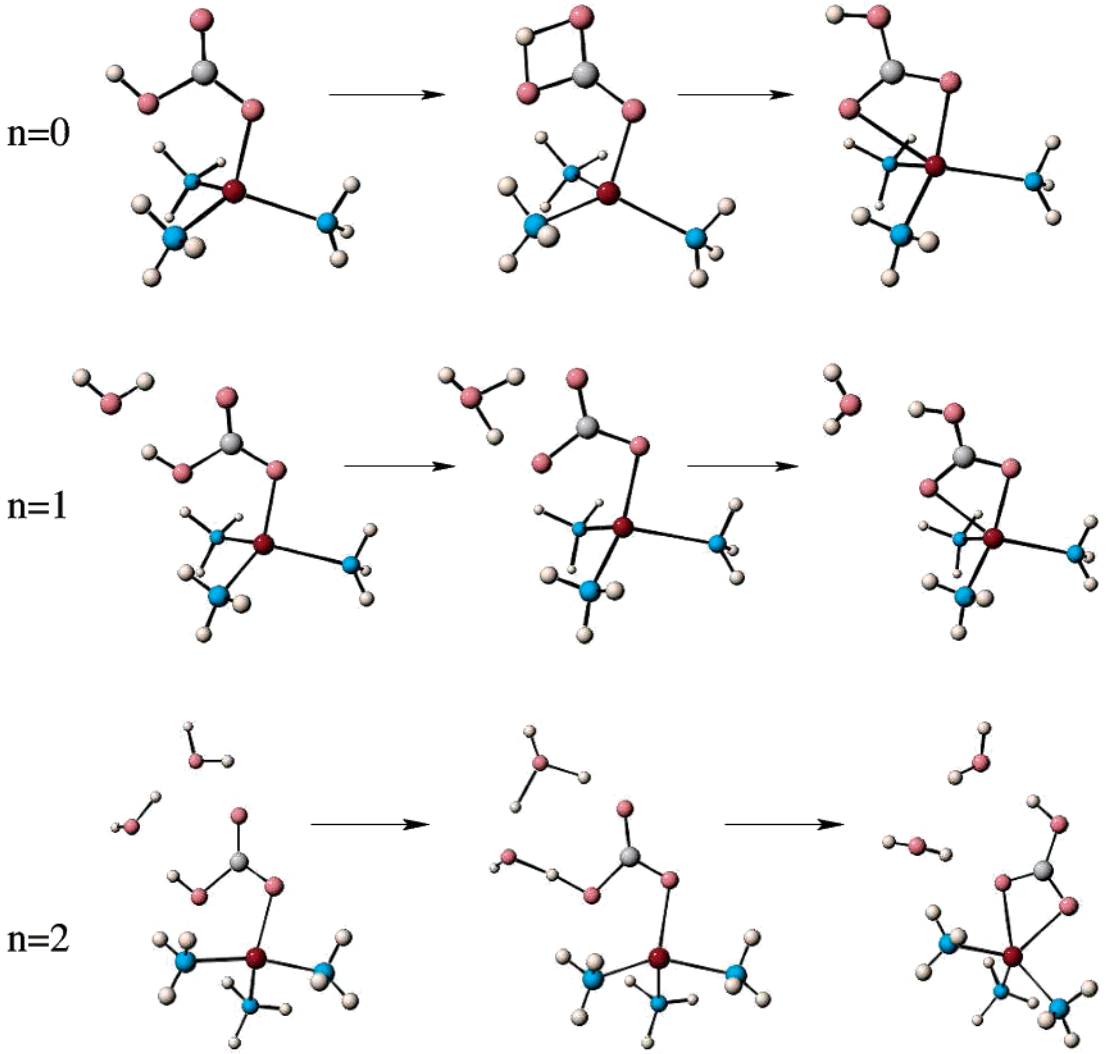

Figure 3. Step in the hydration reaction catalyzed by $n = 0$ (top), $n = 1$ (middle), and $n = 2$ (bottom) water molecules (from left to right, educt, transition state, and product).

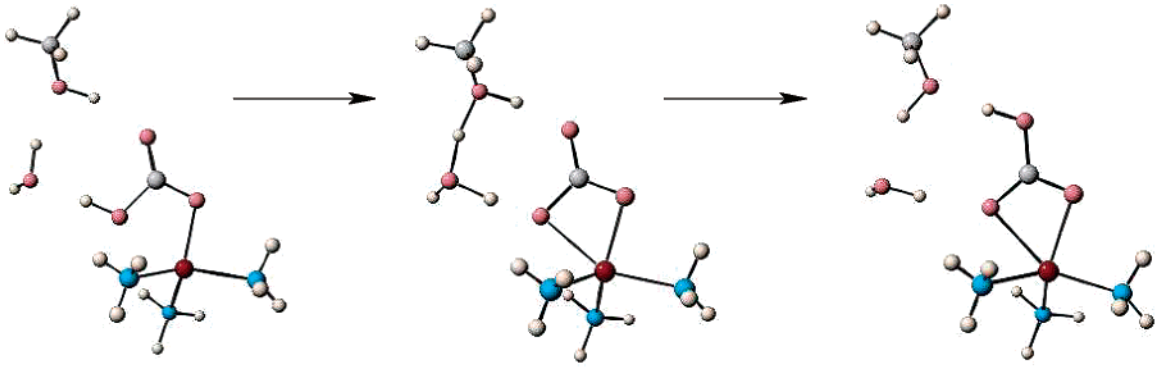

Figure 4. Lipscomb step in the hydration reaction catalyzed by water and methanol, which is used to model the OH-group of Thr199 (from right to left, educt, transition state, and product).

was used as retrieved from the Brookhaven Protein Data Bank[72] (PDB-ID, 2CBA). After addition of hydrogens, 121 TIP3P water molecules were added in a 16 Å sphere around the reactive center by a series of minimizations and high-temperature MD runs until no more water molecules could be added.

3. Results

3.1. Stationary Points—Structures and Energetics. All displayed structures in Figures 3 and 4 were optimized in the course of the energy calculation by the Gaussian-3 method. Coordinates and absolute energies of the stationary points may be found as Supporting Information. The imaginary frequencies were computed at the B3LYP/6-31+G(d) (LanL2DZ with ECPs for Zn) level. The barriers for the forward and backward reactions are displayed in Table 1.

No Catalytical Water Entities. The proton-transfer step of the CO_2 hydration reaction without additional water molecules can be found in Figure 3. The transition state is a strained four-

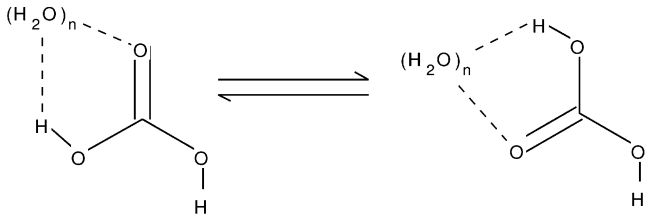

Figure 5. The reference system without $(NH_3)_3Zn^{2+}$ and methanol as catalysts.

membered ring, thus being energetically very unfavorable. The reaction barrier for the hydration reaction is very high (more than 30 kcal/mol), thus ruling out this mechanism for being the catalytically important one. The imaginary frequency is found to be 1923*i* cm^{-1}, which gives a hint that tunneling is very important for this mechanism.

Water as Catalyst. If just one additional water molecule is added as proton mediator, the transition state (see Figure 3), including a six-membered ring, is energetically much more favorable than the transition structure of the uncatalyzed reaction. The energy barrier decreases to 12.1 kcal/mol in the hydration reaction. Still the backward barrier is quite high with 18.0 kcal/mol.

Another additional water molecule (see Figure 3) leads to a transition structure that includes a nearly strainless eight-membered ring. This lowers the barrier to less than 12 kcal/mol in the hydration reaction, but the barrier for the backward reaction is still quite high (even slightly higher than that with one additional water). The imaginary frequency at the transition state is found to be 775*i* cm^{-1}, indicating a broadening of the energy barrier, which means that tunneling becomes less important.

Water and Methanol as Catalysts. Because a further addition of water did not lead to any significant decrease in the reaction barriers, we tried to include the Thr199, which is known to be very important for the catalytic activity of carbonic anhydrase.[13−16,39,40] Because the applied quantum chemical methods are very demanding, it is not feasible to include the whole Thr199; thus, a small molecule as a model of its side chain was employed. We chose methanol to be suitable for this purpose because it is the smallest molecule in which the hydroxy group is attached to a carbon.

Methanol being the only catalytic entity was not considered because the oxygen of Thr199 is too far from the carbon of the bicarbonate (3.5 Å in the crystal structure[12]) to enable a proton transfer all alone. Thus we introduced a water molecule together with the methanol in our model system, as it can be seen in Figure 4. With this combination, the barrier in the hydration reaction drops below 10 kcal/mol and also the barrier for the dehydration of HCO_3^- decreases significantly to about 14 kcal/mol.

3.2. Reference System without Specific Catalysts. To gain information about the importance of various catalytic features of the model system, we have also investigated the intermolecular proton transfer in a similar system but without the $(NH_3)_3Zn^{2+}$ complex and without methanol. The resulting educt system is carbonic acid with the protons in anti−syn conformation (see Figure 5). A similar proton-transfer system with catalytic water entities has already been investigated,[37,38,73−75] but in previous studies, the proton was directed to the oxygen, which was already bound to a hydrogen, leading to the decomposition of carbonic acid. This time, the proton is urged to move to the other oxygen atom, thus yielding again carbonic acid, where the protons are arranged in anti−anti conformation.

TABLE 2: Reaction Barriers (in kcal/mol) for the Proton Transfer in the Reference System without the $(NH_3)_3Zn^{2+}$ Complex and without Methanol as Catalysts at the B3LYP/6-31+G(d) Level of Theory

	forward reaction	backward reaction
+0 H_2O	37.8	39.6
+1 H_2O	13.5	14.7
+2 H_2O	12.1	13.0

The corresponding energy barriers at the B3LYP/6-31+G(d) level of theory are given in Table 2. Coordinates and absolute energies may be found as Supporting Information. Also in the model system, we find a catalytic impact of additional water molecules. The reaction barrier decreases from about 40 kcal/mol to about 12 kcal/mol when two additional water entities are considered.

The lack of the $(NH_3)_3Zn^{2+}$ as a catalyst (as used in our model system for CA II) has strong impacts on the reaction barrier of the forward reaction. The forward barrier of the reference system with the corresponding amount of water entities is 22%−29% higher than that in the model system with the $(NH_3)_3Zn^{2+}$ complex.

These energy values are only used for comparison to the model system, and no kinetic data are derived from them. Thus, we did not calculate any data by high-level methods (such as G2(MP2)) for this reference system.

3.3. Kinetics. With the above-mentioned methods, we determined reaction rates for the various systems, relying on the energy barriers found in Table 1. Values of reaction rates may be found as Supporting Information. As already stated, the investigated proton-transfer step is not the rate-limiting step in the catalytic cycle of carbonic anhydrase. Thus the computed reaction rates of possible proton rearrangement mechanisms should be larger than the experimentally determined turnover number of 10^6 s^{-1} at room temperature; otherwise, they have to be rejected for being too slow. Because we are working with a model system, which is an approximation to the real system, we expect that the neglect of the surrounding protein provides a source of error. Thus the airy rejection of various mechanisms in the enzyme is a difficult task because all we are talking of are the model systems. Nevertheless, similar models have proven to be a valuable source for qualitative information about the mechanistic features in CA II.[21] If a reaction has a turnover that is already larger than 10^6 s^{-1} in the model system, one expects the same mechanism to be even faster in the enzyme because the enzymatic surrounding corresponds to a dielectric constant that is higher than 1, thus presumably stabilizing the transition state, commonly being more polarized than the minima. Thus the energy barriers are expected to decrease when the enzymatic environment is included and as a result the reaction rates are expected to increase.

Figures 6 and 7 show the computed reaction rates. From these plots, one realizes that the uncatalyzed reaction and the reaction catalyzed by just one water molecule can be ruled out as useful mechanisms for being much too slow in comparison to the two other mechanisms in the hydration reaction (see Figure 6). The two other mechanisms, that is, the reaction involving two additional catalytically active molecules (2 H_2O or H_2O and CH_3OH), are both much faster than the rate-limiting step. Therefore both mechanisms can be proposed to occur in CA II at room temperature.

For the backward reaction (i.e., the proton rearrangement step in the dehydration reaction of bicarbonate), the situation changes completely. Figure 7 shows that the mechanism involving

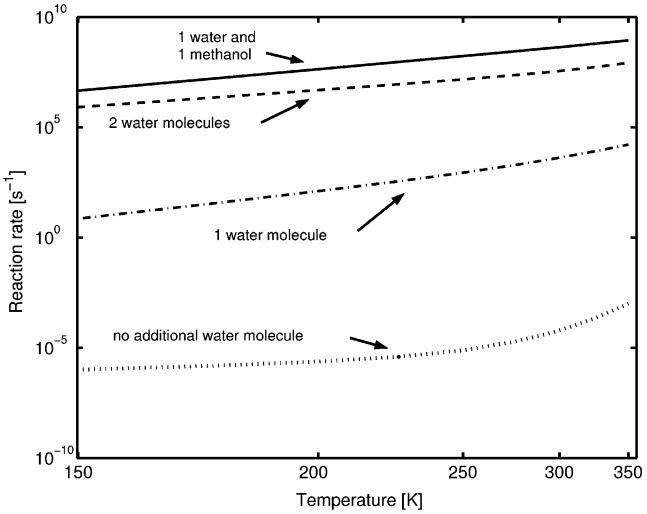

Figure 6. Reaction rates for the proton transfer in the various model systems of CA II in the hydration reaction.

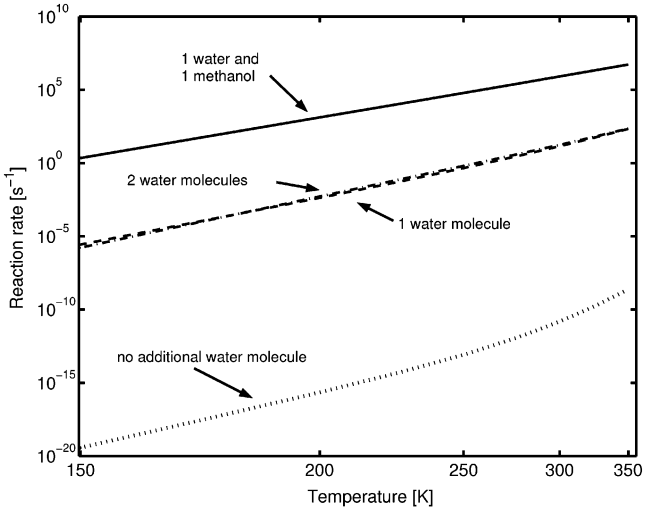

Figure 7. Reaction rates for the proton transfer in the various model systems of CA II in the dehydration reaction.

methanol and water as catalysts leads to reasonable reaction rates at room temperature. This mechanism is 10^5 times faster than the mechanisms in which only water (one or two entities) acts as catalyst. The uncatalyzed mechanism seems to be irrelevant for kinetic reasons.

Contribution of Tunneling. In all discussed mechanisms, we found a significant impact of tunneling, even at room temperature. The uncatalyzed reaction rate includes an enhancement by tunneling by a factor 12 000 at 300 K. This very high transmission coefficient may be explained by the narrow reaction barrier and the small reduced mass corresponding to the transition vector at the transition state. Generally, the reduced mass is very close to 1 (between 1.09 and 1.20) for all four transition states in Figures 3 and 4. This shows that the atomic movement at the transition state is clearly dominated by the protons. Because the tunneling probability crucially depends on the reduced mass along the tunneling path, the low reduced masses enhance the importance of tunneling. The other mechanisms, which involve the concerted movement of two or three protons still reveal an 11−14-fold acceleration of the reaction rate by tunneling. Thus it is shown that tunneling is important in CA II, as it was found to be important in many other enzymes[22,76−78] or in other steps in the catalytic cycle of CA II.[24,28]

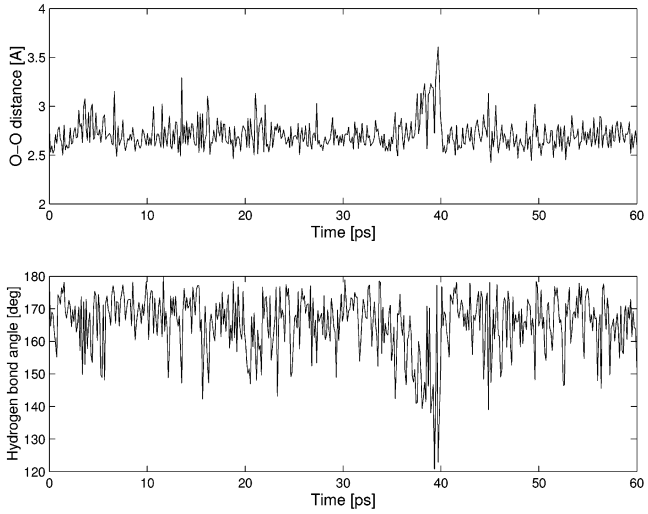

Figure 8. Time evolution in a QM/MM simulation of CA II. Displayed are the distance between the oxygen atoms of the hydrogen bond between Thr199 and Glu106 (upper picture) and the enclosed angle (lower picture). At around 40 ps, the hydrogen bond is broken because of strong fluctuations.

3.4. Simulation Results. The proposed mechanism involving hydrogen transfer via the enzymatic environment requires breakage of the hydrogen bond Thr199-O···Thr199-H···Glu106-O. This hydrogen bond is assumed to be essential for a proper orientation of zinc-bound hydroxide.[39] To gain closer insight in the dynamics of this hydrogen bond, a 60 ps semiempirical QM/MM simulation has been performed. Standard simulation protocols as mentioned in the methods section have been employed. Graphs of the time evolution of the distance between the oxygen atoms of the hydrogen bond, as well as the enclosed angle, can be found in Figure 8.

The distance is below 3 Å for most parts of the simulation, together with enclosed angles between 160° and 180°, which is characteristic for a strong hydrogen bond. However, deviations may occur, as can be found at a time of 40 ps. At this point, the hydrogen bond elongates associated with a significant bending to an almost perpendicular arrangement of 120°. Because such an event has already been observed on a time scale of 40 ps in our simulation, temporary disruption of this hydrogen bond seems feasible. This might constitute the initiation of a catalytic cycle, which promotes the proton transfer in zinc-bound bicarbonate. Moreover, once the hydrogen bond between Thr199 and Glu106 is broken, it may contribute to several catalytic cycles before being reestablished again. Thus, we propose that the hydroxy group of Thr199 is available to participate at the catalytic cycle in the active site of human CA II. Nevertheless proton transfer itself could not be observed in this simulation because the QM region is still quite small (excluding several water entities) and the simulation time is still too short. Enlarging the QM region or prolonging the simulation time is infeasible because the proton transfer is expected to occur once in a time scale of up to 1 μs.

4. Discussion of the Results

In all systems considered (model systems and reference systems), a huge impact of water as a catalyst was found. The inclusion of two additional water entities lowered the reaction barriers to about a third of the barrier of the uncatalyzed proton transfer. The impact of the specific catalyst $(NH_3)_3Zn^{2+}$ may be quantified, when comparing the barriers in the model system with the barriers in the carbonic acid reference system. The zinc

atom apparently lowers the barrier in the forward direction ("forward" means that we refer to the Lipscomb step of the overall hydration reaction of CO_2, whereas "backward" stands for the corresponding step in the dehydration reaction of bicarbonate). The $(NH_3)_3Zn^{2+}$ complex lowers the barrier for the forward reaction by more than 22%. In the backward direction, there is no catalytic effect to be recognized—rather the contrary can be seen: in the model system in Figure 3, the barriers in the backward direction are even slightly higher than those in the reference system. This behavior is the reason Thr199 has to be included in the model system. On inclusion of a water molecule *and* a methanol entity (to model Thr199) in the model system (Figure 4), the barrier for the backward reaction is much lower than in all other cases, when water is the only catalyst (see Table 1). Therefore Thr199 is assumed to be of great importance for the dehydration reaction of bicarbonate. Additionally, the inclusion of methanol also leads, as it is expected, to a decrease in the forward barrier. Altogether, this makes the addition of the $(NH_3)_3Zn^{2+}$ complex and methanol to a powerful catalytic system for the intramolecular proton transfer in bicarbonate. As a justification for the inclusion of methanol in the model system, we performed a semiempirical QM/MM simulation of 50 ps and observed strong fluctuations, which led to the breaking of the hydrogen bond between Thr199 and Glu106. This breaking is the premise for the involvement of the hydroxy group of Thr199 as a proton shuttle in the catalytic cycle of the proton-transfer reaction in CA II.

When observing the reaction rates for the proton transfer, one recognizes again the importance of powerful catalysts in the Lipscomb mechanism. To yield reaction rates that match the experimental turnover numbers of the enzyme reasonably well, one needs to obtain lower barriers than 31 and 40 kcal/mol as they occur in the uncatalyzed system. The zinc-complex catalyst alone does not lead to sufficient acceleration. At least one additional water molecule is needed as a mediator for the moving proton, and for the backward reaction, also a carbon-bound hydroxy group (methanol) must be included to accelerate the reaction rate to values that do not undershoot the experimental rate too strongly. One may argue that we are just working with a model system of CA II, but as already stated, we believe that the inclusion of the enzymatic environment would most likely accelerate the calculated rates by stabilizing the polarized transition states. Thus we yield reaction rates that are clearly much higher than $10^6\ s^{-1}$, and the Lipscomb mechanism seems to be truly feasible for energetic and kinetic reasons. Surely, there is still lack of a kinetic study of the Lindskog mechanism, but our investigation of the Lipscomb mechanism reveals that it is fast enough to be at least a strongly competing mechanism. One advantage of the Lipscomb mechanism is that the movement in the regions of higher energy is nearly restricted to the protons, which leads to the possibility of the enhancement of the reaction rate by tunneling. The Lindskog-type mechanisms include semirotations of the whole bicarbonate entity, where mostly heavy atoms are in movement. Thus we do not expect any significant tunneling contribution in this kind of mechanism.

5. Conclusions

The intramolecular proton transfer in zinc-bound bicarbonate is one very important step in the catalytic cycle in the reversible hydration reaction of CO_2 (i.e., $CO_2 + H_2O \rightleftharpoons HCO_3^- + H^+$) in carbonic anhydrase II (CA II). In a model system, we investigated the influence of various catalysts on the Lipscomb-fashioned proton rearrangement in zinc-bound bicarbonate. It is found that water plays a key role as mediator for the protons and that the reaction rate is strongly accelerated when catalytic water entities are added to the reaction. Further acceleration of the proton-transfer rate (especially in the dehydration reaction of bicarbonate) is observed when a carbon-bound hydroxy group (methanol as a model of Thr199) is included in the system. The availability of the hydroxy group, which requires the breaking of the hydrogen bond between Thr199 and Glu106, was confirmed by a semiempirical QM/MM study of CA II. The electronic barrier for the proton-transfer step in the hydration reaction decreases from more than 30 kcal/mol to less than 10 kcal/mol when one water and one methanol entity are added, forming a nearly strainless eight-membered ring at the transition state. The reaction rate is accelerated by more than 12 orders of magnitude at room temperature by this catalysis, thus being much faster than the experimentally determined rate-limiting step in CA II. In contrast to the Lindskog mechanism, the atomic movement in the regions of higher energy just affects protons, and therefore, tunneling is found to be important by enhancing the reaction rate by at least 1 order of magnitude. Hence, we suggest that the Lipscomb mechanism cannot be ruled out as a realistic proposal for the rearrangement of the zinc-bound bicarbonate in the active site of CA II.

Acknowledgment. C.S.T. acknowledges support by the University of Innsbruck.

Supporting Information Available: Coordinates and absolute energies of the stationary points of the model system and the reference system and values of the reaction rates. This material is available free of charge via the Internet at http://pubs.acs.org.

References and Notes

(1) Maren, T. H. *Physiol. Rev.* **1967**, *47*, 595−781.
(2) Silverman, D. N.; Lindskog, S. *Acc. Chem. Res.* **1988**, *21*, 30−36.
(3) Christianson, D. W.; Fierke, C. A. *Acc. Chem. Res.* **1996**, *29*, 331−339.
(4) Lindskog, S. *Pharmacol. Ther.* **1997**, *74*, 1−20.
(5) Fauci, A. S.; Braunwald, E.; Isselbacher, K. J.; Wilson, J. D.; Martin, J. B.; Kasper, D. L.; Hauser, S. L.; Longo, D. L. *Harrison's Principles of Internal Medicine*, 14th ed.; McGraw-Hill Text: New York, 1998.
(6) Smith, K. S.; Jakubzick, C.; Whittam, T. S.; Ferry, J. G. *Proc. Natl. Acad. Sci. U.S.A.* **1999**, *96*, 15184−15189.
(7) Geers, C.; Gros, G. *Physiol. Rev.* **2000**, *80*, 681−715.
(8) Pocker, Y.; Janjic, N. *J. Am. Chem. Soc.* **1989**, *111*, 731−733.
(9) Eriksson, A. E.; Jones, T. A.; Liljas, A. *Proteins: Struct., Funct., Genet.* **1988**, *4*, 274−282.
(10) Hakansson, K.; Carlsson, M.; Svensson, L. A.; Liljas, A. *J. Mol. Biol.* **1992**, *227*, 1192−1204.
(11) Nair, S. K.; Christanson, D. W. *Eur. J. Biochem.* **1993**, *213*, 507−515.
(12) Xue, Y.; Vidgren, J.; Svensson, L. A.; Liljas, A.; Jonsson, B.-H.; Lindskog, S. *Proteins* **1993**, *15*, 80−87.
(13) Krebs, J. F.; Ippolito, J. A.; Christianson, D. W.; Fierke, C. A. *J. Biol. Chem.* **1993**, *268*, 27458−27466.
(14) Lesburg, C. A.; Christianson, D. W. *J. Am. Chem. Soc.* **1995**, *117*, 6838−6844.
(15) Samuel Toba, G. C.; Merz, K. M., Jr. *J. Am. Chem. Soc.* **1999**, *121*, 2290−2302.
(16) Huang, S.; Sjöblom, B.; Sauer-Eriksson, A. E.; Jonsson, B.-H. *Biochemistry* **2002**, *41*, 7628−7635.
(17) Denisov, V. P.; Jonsson, B.-H.; Halle, B. *J. Am. Chem. Soc.* **1999**, *121*, 2327−2328.
(18) Krebs, J. F.; Fierke, C. A. *Biochemistry* **1991**, *30*, 9153−9160.
(19) Nair, S. K.; Christianson, D. W. *J. Am. Chem. Soc.* **1991**, *113*, 9455−9458.
(20) Scolnick, L. R.; Christianson, D. W. *Biochemistry* **1996**, *35*, 16429−16434.
(21) Sola, M.; Lledos, A.; Duran, M.; Bertran, J. *J. Am. Chem. Soc.* **1992**, *114*, 869−877.
(22) Hwang, J.-K.; Warshel, A. *J. Am. Chem. Soc.* **1996**, *118*, 11745−11751.

(23) Hartmann, M.; Merz, K. M., Jr.; van Eldik, R.; Clark, T. *J. Mol. Model.* **1998**, *4*, 355−365.
(24) Lu, D.; Voth, G. A. *J. Am. Chem. Soc.* **1998**, *120*, 4006−4014.
(25) Muguruma, C. *J. Mol. Struct. (THEOCHEM)* **1999**, *461*−*462*, 439−452.
(26) Mauksch, M.; Bräuer, M.; Weston, J.; Anders, E. *Chem. Biol. Chem.* **2001**, *2*, 190−198.
(27) Bräuer, M.; Perez-Lustres, J. L.; Weston, J.; Anders, E. *Inorg. Chem.* **2002**, *41*, 1454−1463.
(28) Cui, Q.; Karplus, M. *J. Phys. Chem. B* **2003**, *107*, 1071−1078.
(29) Ren, X.; Tu, C.; Laipis, P. J.; Silverman, D. N. *Biochemistry* **1995**, *34*, 8492−8498.
(30) Qian, M.; Tu, C.; Earnhardt, J. N.; Laipis, P. J.; Silverman, D. N. *Biochemistry* **1997**, *36*, 15758−15764.
(31) Earnhardt, J. N.; Qian, M.; Tu, C.; Laipis, P. J.; Silverman, D. N. *Biochemistry* **1998**, *37*, 7649−7655.
(32) An, H.; Tu, C.; Ren, K.; Laipis, P. J.; Silverman, D. N. *BBA*−*Proteins Proteomics* **2002**, *1599*, 21−27.
(33) Vladimir P.; Denisov, B.-H. J.; Halle, B. *J. Am. Chem. Soc.* **1999**, *121*, 2327−2328.
(34) Isaev, A. N. *J. Mol. Struct. (THEOCHEM)* **2002**, *582*, 195−203.
(35) Zheng, Y.-J.; Merz, K. M., Jr. *J. Am. Chem. Soc.* **1992**, *114*, 10498−10507.
(36) Sola, M.; Lledos, A.; Duran, M.; Bertran, J. *Theor. Chim. Acta* **1995**, *91*, 333−351.
(37) Loerting, T.; Tautermann, C.; Kroemer, R. T.; Kohl, I.; Hallbrucker, A.; Mayer, E.; Liedl, K. R. *Angew. Chem., Int. Ed.* **2000**, *39*, 891−894.
(38) Tautermann, C. S.; Voegele, A. F.; Loerting, T.; Kohl, I.; Mayer, E.; Liedl, K. R. *Chem.*—*Eur. J.* **2002**, *8*, 66−73.
(39) Merz, K. M., Jr. *J. Mol. Biol.* **1990**, *214*, 799−802.
(40) Liang, Z.; Xue, Y.; Behravan, G.; Jonsson, B.-H.; Lindskog, S. *Eur. J. Biochem.* **1993**, *211*, 821−827.
(41) Pople, J. A.; Head-Gordon, M.; Fox, D. J.; Raghavachari, K.; Curtiss, L. A. *J. Chem. Phys.* **1989**, *90*, 5622−5629.
(42) Curtiss, L. A.; Jones, C.; Trucks, G. W.; Raghavachari, K.; Pople, J. A. *J. Chem. Phys.* **1990**, *93*, 2537−2545.
(43) Curtiss, L. A.; Raghavachari, K.; Trucks, G. W.; Pople, J. A. *J. Chem. Phys.* **1991**, *94*, 7221−7230.
(44) Curtiss, L. A.; Raghavachari, K.; Redfern, P. C.; Rassolov, V.; Pople, J. A. *J. Chem. Phys.* **1999**, *110*, 4703−4709.
(45) Lee, T. J.; Taylor, P. R. *Int. J. Quantum Chem., Quantum Chem. Symp.* **1989**, *23*, 199−207.
(46) Eyring, H. *J. Chem. Phys.* **1935**, *3*, 107−115.
(47) Garret, B. C.; Truhlar, D. G. *J. Chem. Phys.* **1983**, *79*, 4931−4938.
(48) Truhlar, D. G.; Garrett, B. C. *Annu. Rev. Phys. Chem.* **1984**, *35*, 159−189.
(49) Garrett, B. C.; Joseph, T.; Truong, T. N.; Truhlar, D. G. *Chem. Phys.* **1989**, *136*, 271−283.
(50) Gonzalez-Lafont, A.; Truong, T. N.; Truhlar, D. G. *J. Chem. Phys.* **1991**, *95*, 8875−8894.
(51) Skodje, R. T.; Truhlar, D. G.; Garret, B. C. *J. Phys. Chem.* **1981**, *85*, 3019−3023.
(52) Truhlar, D. G.; Isaacson, A. D.; Garrett, B. C. In *Theory of Chemical Reaction Dynamics*; Baer, M., Ed.; CRC Press: Boca Raton, FL, 1985; Chapter Generalized Transition State Theory, pp 65−137.
(53) Tucker, S. C.; Truhlar, D. G. In *New Theoretical Concepts for Understanding Organic Reactions*; Bertran, J., Csizmadia, I. G., Eds.; Kluwer Academic Publishers: Dortrecht, The Netherlands, 1989; Chapter Dynamical formulation of transition state theory: Variational transition states and semiclassical tunneling, pp 291−346.
(54) Jursic, B. S. *J. Mol. Struct. (THEOCHEM)* **1997**, *417*, 89−94.
(55) Page, M.; McIver, J. W. *J. Chem. Phys.* **1988**, *88*, 922−935.
(56) Melissas, V. S.; Truhlar, D. G.; Garrett, B. C. *J. Chem. Phys.* **1992**, *96*, 5758−5772.
(57) Hu, W.-P.; Liu, Y.-P.; Truhlar, D. G. *J. Chem. Soc., Faraday Trans.* **1994**, *90*, 1715−1725.
(58) Child, M. *Semiclassical Mechanics with Molecular Applications*; Clarendon Press: Oxford, U.K., 1991.
(59) Skodje, R. T.; Truhlar, D. G. *J. Chem. Phys.* **1982**, *77*, 5955−5976.
(60) Baldridge, K. K.; Gordon, M. S.; Steckler, R.; Truhlar, D. G. *J. Phys. Chem.* **1989**, *93*, 5107−5119.
(61) Konkoli, Z.; Kraka, E.; Cremer, D. *J. Phys. Chem. A* **1997**, *101*, 1742−1757.
(62) Fernandez-Ramos, A.; Truhlar, D. G. *J. Chem. Phys.* **2001**, *114*, 1491−1496.
(63) Liu, Y.-P.; Lu, D.-H.; Gonzalez-Lafont, A.; Truhlar, D. G.; Garrett, B. C. *J. Am. Chem. Soc.* **1993**, *115*, 7806−7817.
(64) Frisch, M. J.; Trucks, G. W.; Schlegel, H. B.; Scuseria, G. E.; Robb, M. A.; Cheeseman, J. R.; Zakrzewski, V. G.; Montgomery, J. A., Jr.; Stratmann, R. E.; Burant, J. C.; Dapprich, S.; Millam, J. M.; Daniels, A. D.; Kudin, K. N.; Strain, M. C.; Farkas, O.; Tomasi, J.; Barone, V.; Cossi, M.; Cammi, R.; Mennucci, B.; Pomelli, C.; Adamo, C.; Clifford, S.; Ochterski, J.; Petersson, G. A.; Ayala, P. Y.; Cui, Q.; Morokuma, K.; Malick, D. K.; Rabuck, A. D.; Raghavachari, K.; Foresman, J. B.; Cioslowski, J.; Ortiz, J. V.; Stefanov, B. B.; Liu, G.; Liashenko, A.; Piskorz, P.; Komaromi, I.; Gomperts, R.; Martin, R. L.; Fox, D. J.; Keith, T.; Al-Laham, M. A.; Peng, C. Y.; Nanayakkara, A.; Gonzalez, C.; Challacombe, M.; Gill, P. M. W.; Johnson, B. G.; Chen, W.; Wong, M. W.; Andres, J. L.; Head-Gordon, M.; Replogle, E. S.; Pople, J. A. *Gaussian 98*, revision A.7; Gaussian, Inc.: Pittsburgh, PA, 1998.
(65) Chuang, Y.-Y.; Corchado, J. C.; Fast, P. L.; Villá, J.; Coitiño, E. L.; Hu, W.-P.; Liu, Y.-P.; Lynch, G. C.; Nguyen, K. A.; Jackels, C. F.; Gu, M. Z.; Rossi, I.; Clayton, S.; Melissas, V. S.; Steckler, R.; Garrett, B. C.; Isaacson, A. D.; Truhlar, D. G. *POLYRATE*, version 8.5; University of Minnesota: Minneapolis, MN, 2000.
(66) Corchado, J. C.; Coitiño, E. L.; Chuang, Y.-Y.; Truhlar, D. G. *Gaussrate 8.5*; University of Minnesota: Minneapolis, MN, 2000.
(67) MacKerell, A. D.; Bashford, D.; Bellott, M.; Dunbrack, R. L.; Evanseck, J. D.; Field, M. J.; Fischer, S.; Gao, J.; Guo, H.; Ha, S.; Joseph-McCarthy, D.; Kuchnir, L.; Kuczera, K.; Lau, F. T. K.; Mattos, C.; Michnick, S.; Ngo, T.; Nguyen, D. T.; Prodhom, B.; Reiher, W. E., III; Roux, B.; Schlenkrich, M.; Smith, J. C.; Stote, R.; Straub, J.; Watanabe, M.; Wiorkiewicz-Kuczera, J.; Yin, D.; Karplus, M. *J. Phys. Chem. B* **1998**, *102*, 3586−3616.
(68) Brooks, C. L., III; Karplus, M. *J. Mol. Biol.* **1988**, *208*, 159−181.
(69) Levy, R. M.; Karplus, M.; McCammon, J. A. *Chem. Phys. Lett.* **1979**, *65* (1), 4−11.
(70) Brooks, C. L., III; Karplus, M. *J. Chem. Phys.* **1983**, *79*, 6312−6325.
(71) Brooks, C. L., III; Bruenger, A.; Karplus, M. *Biopolymers* **1985**, *24*, 843−865.
(72) Berman, H. M.; Westbrook, J.; Feng, Z.; Gilliland, G.; Bhat, T. N.; Weissig, H.; Shindyalov, I. N.; Bourne, P. E. *Nucleic Acids Res.* **2000**, *28*, 235−242.
(73) Liang, J.-Y.; Lipscomb, W. N. *Biochemistry* **1987**, *26*, 5293−5301.
(74) Liang, J. Y.; Lipscomb, W. N. *Int. J. Quantum Chem.* **1989**, *36*, 299−312.
(75) Nguyen, M. T.; Raspoet, G.; Vanquickenborne, L. G.; Van Duijnen, P. T. *J. Phys. Chem. A* **1997**, *101*, 7379−7388.
(76) Kohen, A.; Klinman, J. P. *Acc. Chem. Res.* **1998**, *31*, 397−404.
(77) Alhambra, C.; Gao, J.; Corchado, J. C.; Villà, J.; Truhlar, D. G. *J. Am. Chem. Soc.* **1999**, *121*, 2253−2258.
(78) Kohen, A.; Cannio, R.; Bartolucci, S.; Klinman, J. P. *Nature* **1999**, *399*, 496−499.